Article

tREPs—A New Class of Functional tRNA-Encoded Peptides

Amrita Chakrabarti, Monika Kaushik, Juveria Khan, Deepanshu Soota, Kalairasan Ponnusamy, Sunil Saini, Siddharth Manvati, Jhalak Singhal, Anand Ranganathan, Soumya Pati,* Pawan Kumar Dhar,* and Shailja Singh*

Cite This: *ACS Omega* 2022, 7, 18361−18373

Read Online

ACCESS | 📊 Metrics & More | 📰 Article Recommendations | 🔵 Supporting Information

ABSTRACT: We asked if transfer RNA (tRNA) ever got an opportunity of translating its own sequence during evolution, what would have been the function of such tRNA-encoded peptides (tREPs)? If not, could one artificially synthesize tREPs to study the corresponding functional outcomes? Here, we report a novel, first-in-the-class, chemically synthesized tREP-18 molecule originating from the *Escherichia coli* tRNA sequence showing potent antileishmanial property. As a first step, *E. coli* tRNAs were computationally translated into peptide sequence equivalents and a database of full-length hypothetical tREPs was created. The tREP sequences were sent into sequence, structure, and energy filters to narrow down potential peptides for experimental validation. Based on the functional predictions, tREPs were screened against antiparasitic targets, leading to the identification of tREP-18 as a potential antiparasitic peptide. The in vitro assay of chemically synthesized tREP-18 on the *Ag83* strain of *Leishmania donovani* showed its potent antileishmanial property (IC50 value of 22.13 nM). The atomic force microscopy and scanning electron microscopy images indicated significant alteration in the cytoskeletal architecture of tREP-18-treated parasites. Also, tREP-18 seems to destabilize the mitochondrial membrane potential of parasites, disrupting their cellular integrity and leading to parasitic death. The cellular assays of the tREP-18 peptide on the BS12 strain, a clinical isolate of post-kala azar dermal leishmaniasis, demonstrated its significant efficacy at an IC50 value of 15 nM. The tREP-18 peptide showed a toxic effect on the amastigote stage of the parasite, showing macrophage pathogen clearance at a concentration of 22.5 nM. This study provides the proof of the concept of making a new class of functional peptides from tRNA sequences. It also opens a huge untapped tRNA-peptide space toward novel discoveries and applications. In the future, it would be interesting to perform tREP edits and redesign tREPs toward specific applications.
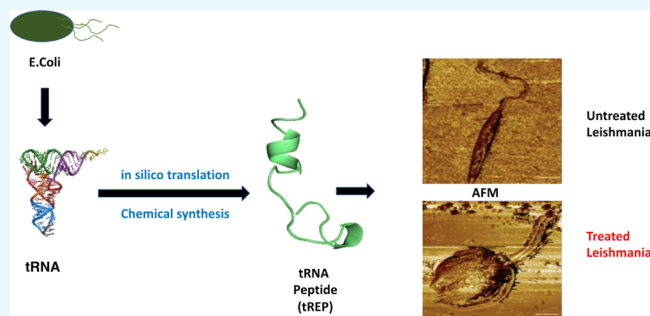
1. INTRODUCTION

Transfer RNAs (tRNAs) are small non-coding RNAs (76−90 nucleotides in length) that ferry amino acids to the ribosomal interface for constructing specific polypeptide chains.[1] To explain their origin and evolution, models have been proposed to imply direct duplication and evolution of RNA hairpin encoding genes[2] and co-evolution of primordial tRNA with their association to translation machinery.[3]

Furthermore, disrupted tRNA genes have been reported in the form of intron-containing tRNA,[4] split tRNA,[5,6] and permuted tRNA in archaea.[7] The evolutionary reasons behind these unexpected forms of tRNA gene sequences are unclear.[8] The asymmetric combinations of tRNA halves have been postulated to generate tRNA diversity.[9] Recent evidence has shown that tRNA-derived small RNAs are generated following cleavage at specific sites by distinct nucleases and have multiple biological functions.[10] However, no study has ever exploited the translation of tRNAs and/or the biological significance of tRNA-derived peptides. To address these unsolved puzzles and exploit their therapeutic implications, we decided to design novel tRNA-based peptides and screen them against visceral leishmaniasis and its convoluted form, post-kala-azar dermal leishmaniasis (PKDL). Both of these disease manifestations are caused by the species of the protozoan obligate parasite, genus Leishmania (Kinetoplastida, Trypanosomatidae), which is usually anthroponotic in origin and transmitted by the bite of female phlebotomine sand flies. Globally, an estimated 0·7−1 million newly reported cases of leishmaniasis emerge every year from the 100 endemic countries. Thus, there is a requirement to develop new potent antileishmanials that are less prone to resistance development. Toward this, for the first time, we identified a novel membrane binding peptide that was in silico translated from tRNA of the *Escherichia coli* genome with superb antiparasitic activities. This finding opened a new

horizon for the better acceptance of peptides as a drug modality against leishmaniasis. To achieve this aim, the structure of hypothetical peptides was computationally predicted, followed by (a) the chemical synthesis of lead peptides, (b) experimental determination of their possible function(s), and (c) evaluation of cellular footprints for their functional property.

We have established a novel combinatorial approach involving in silico analysis tools and synthetic biology applications to characterize prokaryotic tRNA variants from the mg1655 strain of *E. coli*. Based on computational biology and structural analyses, we finally synthesized **tREP-18** as the lead peptide following screening against an antiparasitic database. The tREP-18 showed strong potency against the laboratory and clinical strains of *Leishmania donovani* at 40 and 15 nM ($\geq$IC50) concentrations, respectively, while mammalian cells were found to be absolutely tolerant to the presence of **tREP-18** in the mM range. Importantly, the **tREP-18** peptide was efficient at reducing amastigote cell viability within a macrophage at a minimal concentration of 22.5 nM. Precisely, the peptide targeted both the stages of the parasite competently. This work has provided novel insight into noncanonical applications of prokaryotic tRNA and laid a sound foundation for future development of tRNA-derived antileishmanial peptides.

2. MATERIALS AND METHODS

2.1. Bioinformatics-Based Novel Peptide Screening.
We retrieved the tRNA gene sequences of *E. coli* strain K-12 sub-strain MG1655, from the genomic tRNA database that contained tRNA genes. 87 tRNA gene sequences were retrieved and computationally translated into protein sequences using the Transeq tool[11] of the European Bioinformatics Institute (https://www.ebi.ac.uk/Tools/st/emboss_transeq/). Each tRNA sequence was then translated into protein sequences and the sequences with stop codons were removed. Furthermore, we computationally modeled the three-dimensional (3D) structure of the peptide using the Phyre server[12] (http://www.sbg.bio.ic.ac.uk/phyre2/). The modeled structures were energy minimized and validated using GROMACS 5.1[13] (https://www.gromacs.org/) and PROCHECK[14] (https://www.ebi.ac.uk/thornton-srv/software/PROCHECK/), respectively. To filter the most stable peptide, we subjected the models to FOLDX-based stability analysis[15] (https://foldxsuite.crg.eu/). The stable peptides were screened against the antiparasite peptide database[16] (http://crdd.osdd.net/raghava/parapep/). The peptides with high similarity in the database were considered for experimental validation such as tREP-18. Based on the minimum *E*-value obtained, tREP-18 was further chosen for estimating its binding efficacy with the lipid bilayer using the orientation of proteins on membrane (OPM) server[17] (http://opm.phar.umich.edu) that shows the spatial arrangements of peptides with respect to the hydrocarbon core of the lipid bilayer. To design a negative control for these two peptides, we have generated a scrambled peptide using the Phypre server by changing aspartic acid and glutamic acid at the 7th and 20th positions to proline.

2.2. Parasite Culturing and Treatment.
The promastigote form of *L. donovani* (Ag83 strain) was cultured at 26 °C in M199 media (GIBCO, India) pH 7.4 supplemented with 10% (v/v) inactivated fetal bovine serum (FBS) (GIBCO, India) and 0.02 mg/mL gentamycin (Life Technologies, USA). *L. donovani* BS12 strain, a clinical isolate of PKDL, was obtained as a kind gift from Dr. Mitali Chatterjee (Institute of Post-Graduate Medical Education and Research and Seth Sukhlal Karnani Memorial Hospital, Kolkata, India). These isolates were routinely cultured at 22 °C in modified M199 medium (GIBCO, India) with 100 U/mL penicillin−streptomycin (Gibco, Invitrogen, Thermo Fisher Scientific, NY), 8 μM hemin (4 mM stock made in 50% triethanolamine) (Sigma, USA), and 25 mM *N*-[2-hydroxyethyl]piperazine-N0-[2-ethanesulfonic acid] (Sigma), supplemented with 10% heat inactivated FBS.[18,19] The strain in cultures was maintained between 10^6 and 10^7 cells/mL for continuous exponential growth in the BSL2 laboratory facility. 1×10^6 cells/mL of parasite count was constantly maintained for all the experiments. **tREP-18** and scrambled peptides, respectively, were resuspended in dimethyl sulphoxide (Sigma-Aldrich) for the preparation of a 1 M stock solution. The working concentrations for **tREP-18** were varied, ranging from 1 to 40 nM. Following IC50 calculation, higher concentrations of the peptide were chosen for performing all in vitro experiments at different time intervals. Parasites without any inhibitor treatment were maintained as negative controls.

2.3. Cellular Viability of J774.A1 Cells.
The J774.A1 murine macrophage cell line was grown in Roswell Park Memorial Institute (RPMI) 1640 medium in the presence of 10% (v/v) FBS with 100 U/mL penicillin−100 μg/mL streptomycin (Gibco, Invitrogen, Thermo Fisher Scientific, NY) at 37 °C (humidified) and 5% CO_2. The cells were seeded in 96-well plates at a seeding density of 30 000 cells/well and allowed to adhere overnight at 37 °C. Adhered cells were treated with **tREP-18** and scrambled peptides in a dose-dependent manner for 24 h. Control was maintained without the addition of any peptide. Cytotoxic effects were assessed using the 3-[4,5- dimethylthiazol-2-yl]-2,5-diphenyl tetrazolium bromide (MTT) assay kit (Sigma-Aldrich). The conversion of MTT to formazan crystals by viable cells was measured at 595 nm. The J774.A1 murine macrophage cell line was a kind gift from Prof. Rentala Madhubala's laboratory at the School of Life Sciences, JNU, New Delhi.

2.4. Cytotoxicity Assay by LDH.
The lactate dehydrogenase (LDH) cytotoxic assay was performed as per standard protocol (CytoTox 96 Non-Radioactive Cytotoxicity Assay-Promega, USA). Initially, promastigotes of the Ag83 strain and the BS12 strain of PKDL were suspended into a 96-well microtiter plate (100 μL well volume). For calculating IC50, parasite samples in triplicates were exposed to various concentrations (1−100 nM) of both **tREP-18** peptides at 26 °C for 24 h. Colorimetric quantification of toxicity toward promastigotes upon treatment with various concentrations of the peptides was carried out using the LDH assay. Further percentage growth inhibition was calculated using the formula

$$\% \textbf{ inhibition} = \frac{\textbf{peptide treated LDH activity} - \textbf{spontaneous LDH activity}}{\textbf{maximum LDH activity} - \textbf{spontaneous LDH activity}} \times 100$$

As per the formula, the spontaneous LDH activity = activity of the untreated cells, and the maximum LDH activity = activity of the amphotericin B-treated cells. These values were transferred to the GraphPad Prism version 8.0.1, and the IC50 value for tREP-18 was generated for the Ag83 and PKDL strains of *L. donovani* using a sigmoidal dose−response model with the nonlinear regression tool. The time-dependent cytotoxicity of tREP-18 was also examined with log phase promastigotes (1×10^6/mL) of the Ag83 strain and the BS12

strain of PKDL, respectively. The parasite samples in triplicates were exposed to various concentrations (1−40 nM) of tREP-18 and incubated at 26 °C for 24, 48, and 72 h, respectively. Amphotericin B (3 μg/mL) (Sigma-Aldrich)-treated parasites were used as the positive control in in vitro assays. Finally, the percentage cytotoxicity of **tREP-18** was calculated by normalizing with an amphotericin B treatment that rendered 100% cytotoxicity. Promastigotes were also treated with scrambled peptides and their cytotoxicity on parasites was evaluated for 24, 48, and 72 h, respectively, by the LDH assay as described in the previous experiment. The untreated log phase of promastigotes (1 × 10^6/mL) was maintained as negative controls.

2.5. Apoptotic Assay. *L. donovani* Ag83 promastigotes undergoing apoptosis in both treated and untreated samples were measured by propidium iodide (PI) staining. After exposure to the peptide for a period of 72 h, cells were harvested, phosphate-buffered saline (PBS) washed and stained with PI (5 μg/mL) (Life Technologies, USA). This was followed by an incubation period of 20 min at 37 °C. Subsequently, cells were washed for excessive stain removal and resuspended in 250 μL of PBS. Cells were further analyzed through BD FACS Diva and visualized using a fluorescence microscope with a 510−560 nm filter block for the detection of PI red fluorescence.

2.6. Morphological Study of Promastigotes by Scanning Electron Microscopy. A morphological study of **tREP-18**-treated promastigotes was examined by scanning electron microscopy (SEM). Sample preparation for SEM was carried out with slight modification in the protocol.[20] Cells were incubated with 40 nM of **tREP-18** for 72 h at 26 °C. These promastigotes were then harvested at 1100 g for 15 min at room temperature (RT), followed by the addition of fresh media. EM-grade glutaraldehyde was directly added to the cells containing M199 media to a final concentration of 2.5% glutaraldehyde (from a 25% stock of EM-grade glutaraldehyde). The cells were centrifuged for 10 min at 800g and the media was removed. Promastigotes were then resuspended in 0.1 M phosphate buffer (pH 7.2) and washed twice. These promastigotes were further fixed with 2.5% (v/v) glutaraldehyde in the same buffer for 120 min. Glass coverslips were cleaned with ethanol followed by immersion in a 0.1% (w/v) solution of poly-L-lysine (sigma) in water. Coverslips were then rinsed in water and left to air-dry in the laminar hood. A 200 μL of cell suspension was added to each coverslip, ensuring the coverslip was completely covered by the cell suspension. Next, these coverslips were placed in individual wells of a 12-well tissue culture plate. This plate was left for 10 min at RT for the cells to settle down and adhere to the coverslips. The adherence was checked using a Nikon inverted microscope (Eclipse Ts2-FL, USA). Samples were then post fixated in 1% osmium tetroxide for 1 h and dehydrated by gradient acetone concentration (50−100%) for 20 min each. Thereafter, samples were treated with 100% hexamethyldisilane at RT for 5 min and mounted on aluminum stubs with adhesive carbon tape. Prior to SEM application, a thin gold layer was coated by means of a sputter coater (SC7640, Polaron Equipment, England, U.K). The samples were observed under an environmental, variable pressure scanning electron microscope (Carl Zeiss EV0-40, Cambridge, U.K.) at a voltage of 20 kV and a working distance of 10 mm.

2.7. Study of Surface Topology of tREP-18-Treated *L. donovani* Promastigotes Using Atomic Force Micros-copy. Sample preparation for the atomic force microscopy (AFM) analysis was carried out as per the standard protocol.[21] Cells were incubated with 40 nM of the peptide for 72 h at 26 °C. These promastigotes were then harvested by centrifugation at 1100g for 15 min at RT, washed with 0.1 M phosphate buffer (pH 7.2), and fixed with 2.5% (v/v) glutaraldehyde in the 0.1 M phosphate buffer for 1 h. Cells were washed using the phosphate buffer and overlaid onto poly-L-ornithine (Sigma)-coated microslides having a dimension of 10 mm × 10 mm. Samples were then washed twice in molecular biology grade water (Sigma) and dried in laminar hood airflow. Scanning of promastigote cells was carried out using a TT-AFM atomic force microscope. A 50 μm scanner was used, and the instrument operation was performed in the tapping and noncontact mode. Image details were calculated using XEI software in first-order flattened 20 × 20 μm^2 areas in the center of the cell body.

2.8. Quantification of Mitochondrial Membrane Potential. Mitochondrial membrane ($\Delta\psi$m) potential was assessed using flow cytometry and fluorescence microscopy-based analyses with 5,6-dichloro-2-[3-(5,6-dichloro-1,3-diethyl-1,3-dihydro-2H-benzimidazol-2-ylidene)-1propenyl]-1,3-diethyl-iodide (JC-1) (Life Technologies, USA) as a probe. The range of concentration from 4 to 40 nM of the peptide was used for treatment. Treated and untreated groups were incubated for a period of 24 h. Parasites were washed with PBS, the JC-1 probe was added to a 6 μM final concentration, and samples were analyzed using BD FACS Diva. The labeled cells were also allowed to adhere to the glass slides for visualization under the Nikon Ti-DH eclipse fluorescence microscope (USA). The approximate fluorescence excitation/emission maxima of 514/529 nm for the monomeric form and 585/590 nm for the J-aggregate form were used.

2.9. Promastigote Proliferation Assay. Cell growth and multiplication were assessed by flow cytometry and fluorescence microscopy with 6-carboxyfluorescein diacetate succinimidyl ester (CFDA-SE, Life Technologies, USA) as a probe. Ag83 parasites were washed thrice with 0.1 M PBS. The cells were labeled with 2.8 μg/mL CFDA-SE dye and incubated at 37 °C for 10 min with 3 to 4 times of intermittent mixing. Following this, cells were resuspended in ice-cold M199 medium and later centrifuged at 1200g for 10 mins (4 °C). The pellet was then suspended in fresh medium. Cells were treated with the peptide at different concentrations and were analyzed using a flow cytometer (BD FACS DIVA) for three consecutive replicates at 24 and 48 h. The labeled cells were also allowed to adhere to glass slides for visualization under the Nikon TI-DH eclipse fluorescence microscope (USA). Fluorescence intensity was determined using an excitation filter at 485 nm and an emission filter at 535 nm. The number of parasites was also determined by staining with trypan blue every 24 h for a period of 72 h. Quantification of the viable parasites was determined by counting the parasites with the clear cytoplasm (non-stained) using a Neubauer hemocytometer with a coverslip. Three independent experiments were performed, and the data were expressed as the mean ± standard deviation (SD).

2.10. Effect of tREP-18 Peptide Against Intracellular Amastigotes. The J774.A1 murine macrophage cell line was plated at a cell density of 5 × 10^5 cell well^{-1} in a six-well flat bottom plate. For infection, late-stage *L. donovani* rich in metacyclic promastigotes was added at a ratio of 10:1 along with the peptide of interest. After 12 h, uninfected
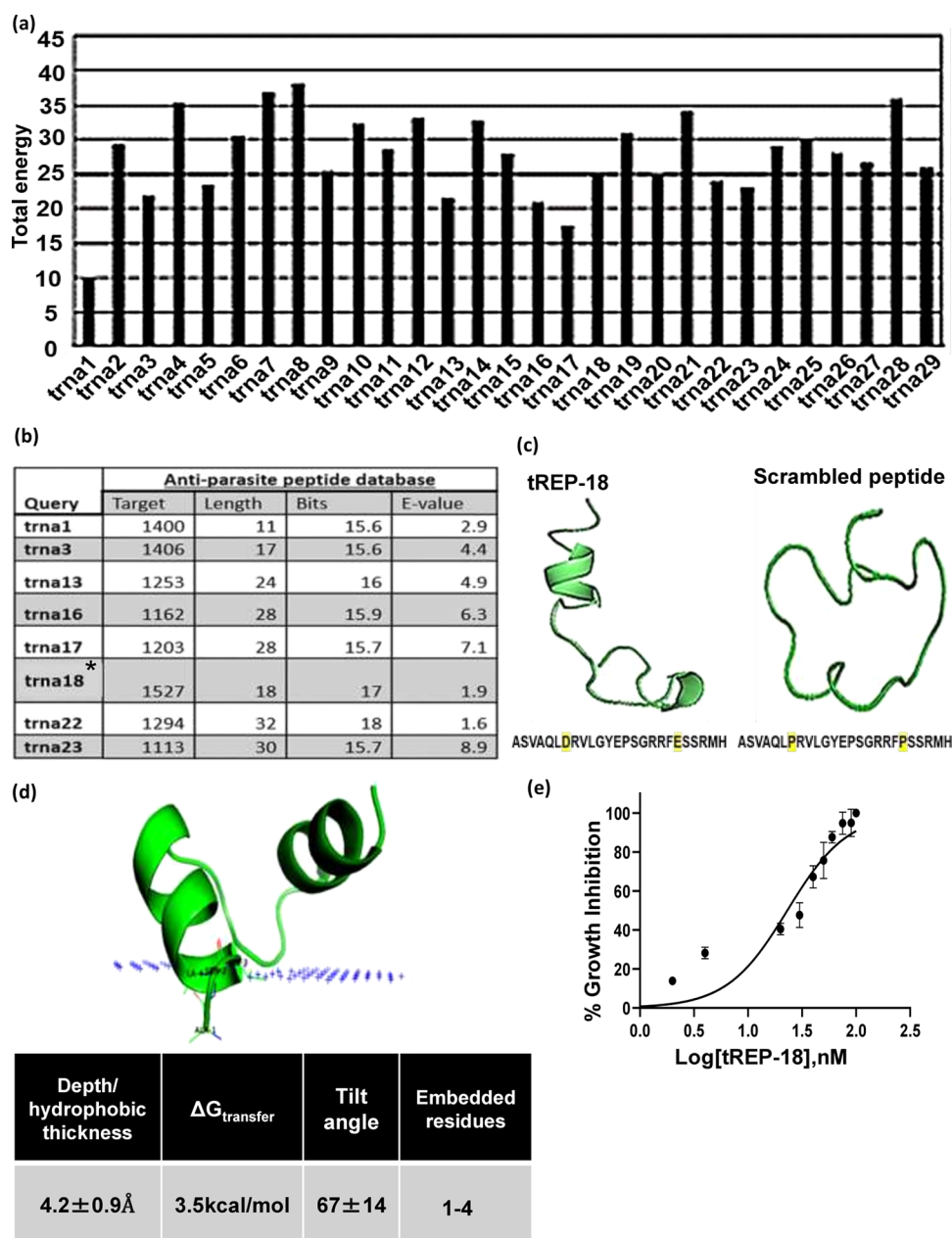
Figure 1. Structural stability analysis of t-RNA peptides along with in silico screening against the antiparasite peptide database and their inhibitory effect on promastigotes. (a) Graphical representation total free energy values of t-RNA peptides depicted stability of their high-resolution 3D structures; (b) table represented filtered sequence similarity profiles of tRNA peptides based on screening against the antiparasitic peptide database; (c) **representative** 3D structures of tREP-18 and the scrambled peptide revealed the presence of an α-helix and a turn in tREP-18 while the scrambled peptide showed random coiling; (d) membrane binding affinity of the tREP-18 peptide was found to be in a moderate range, given the minimum depth/hydrophobic thicknesss is 1 Å; (e) percentage inhibition of promastigotes treated with the tREP-18 peptide was evaluated at 24 h using the LDH assay and plotted as a sigmoidal curve. Data normalization was performed by taking into consideration the cytotoxicity induced by the positive control (amphotericin B-3 μg/mL) as 100%. IC50 values for promastigotes of the Ag83 strain were analyzed using GraphPad Prism, represented as the mean $\pm$ SD where $n = 3$, independent experiments.

promastigotes were washed off with PBS. Infected macrophages were treated with the tREP-18 peptide at nearly an IC50 concentration and incubated for 72 h. Amphotericin B was taken as a positive control. After incubation, visualization and counting of intracellular parasite load were performed using Giemsa staining (Sigma-Aldrich).

2.11. Statistical Analysis. Student's t-test was applied to evaluate significant differences between treatment and control samples in all the experiments performed using the analysis of variance (ANOVA) test. The P-value < 0.05 and p-value < 0.01 were considered to be significant (indicated as * and **, respectively). Results represent the mean $\pm$ SD of a minimum of three independent experiments. The calculated IC_{50} value and all the statistical analyses were performed using GraphPad Prism version 8.01.

3. RESULTS

3.1. In Silico Retrieval, Translation of tREPs from *E. coli* Genome, and Evaluation of the Cytotoxic Effect of Lead tREP. A total of 87 tRNAs from the *E. coli* tRNA
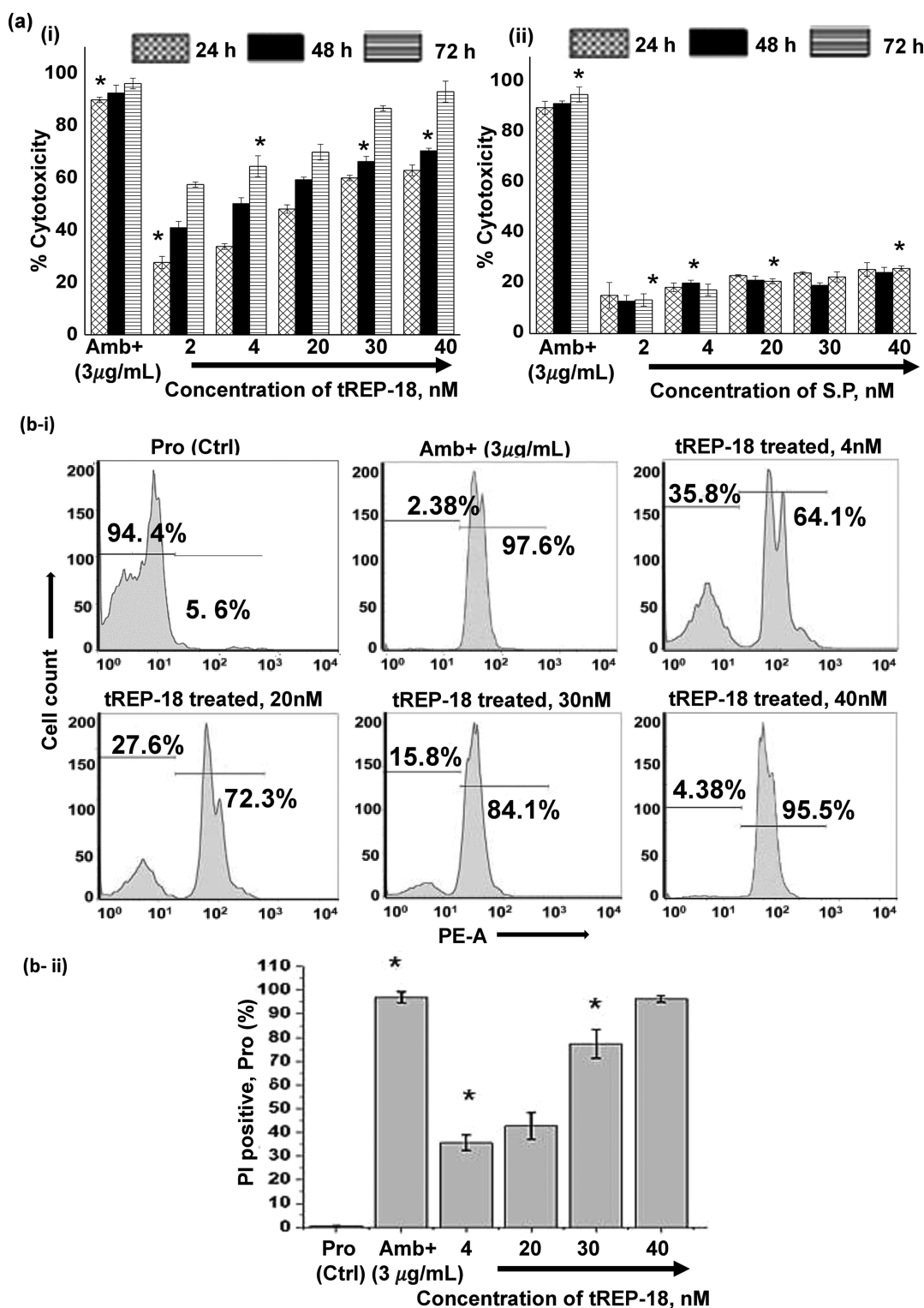
Figure 2. Elucidation of tREP-18 on the metabolic cell viability of promastigotes, [a(i)] Bar graph represented LDH release by tREP-18-treated promastigotes in the dose- and time-dependent manner, with a maximum effect at 40 nM for 72 h; [a(ii)] treatment of scrambled peptides in promastigotes demonstrated non-cytotoxic effects at 72 h; [b(i)] flow cytometry histograms demonstrated the significant death of parasites at 72 h following peptide treatment (Pro refers to promastigotes); [b(ii)] tREP-18 treatment at 40 nM of concentration showed 95.5% of PI positivity in promastigotes at 72 h; the graph represents the mean ± SD of minimum $n = 3$ independent experiments performed using ANOVA test for all the assays, *p-value < 0.05 was considered significant.

database were retrieved and computationally translated into corresponding amino acid equivalents. Of these, 60 translated sequences showed one or more stop codons and were discarded [Table S1]. The remaining 29 full-length peptides

were then finalized into two peptides, namely tREP-18 and tREP-22, based on in silico analyses. The selection was based on their total energy with a minimum E-value [Figure 1a], length of sequence, and structural resemblance with the
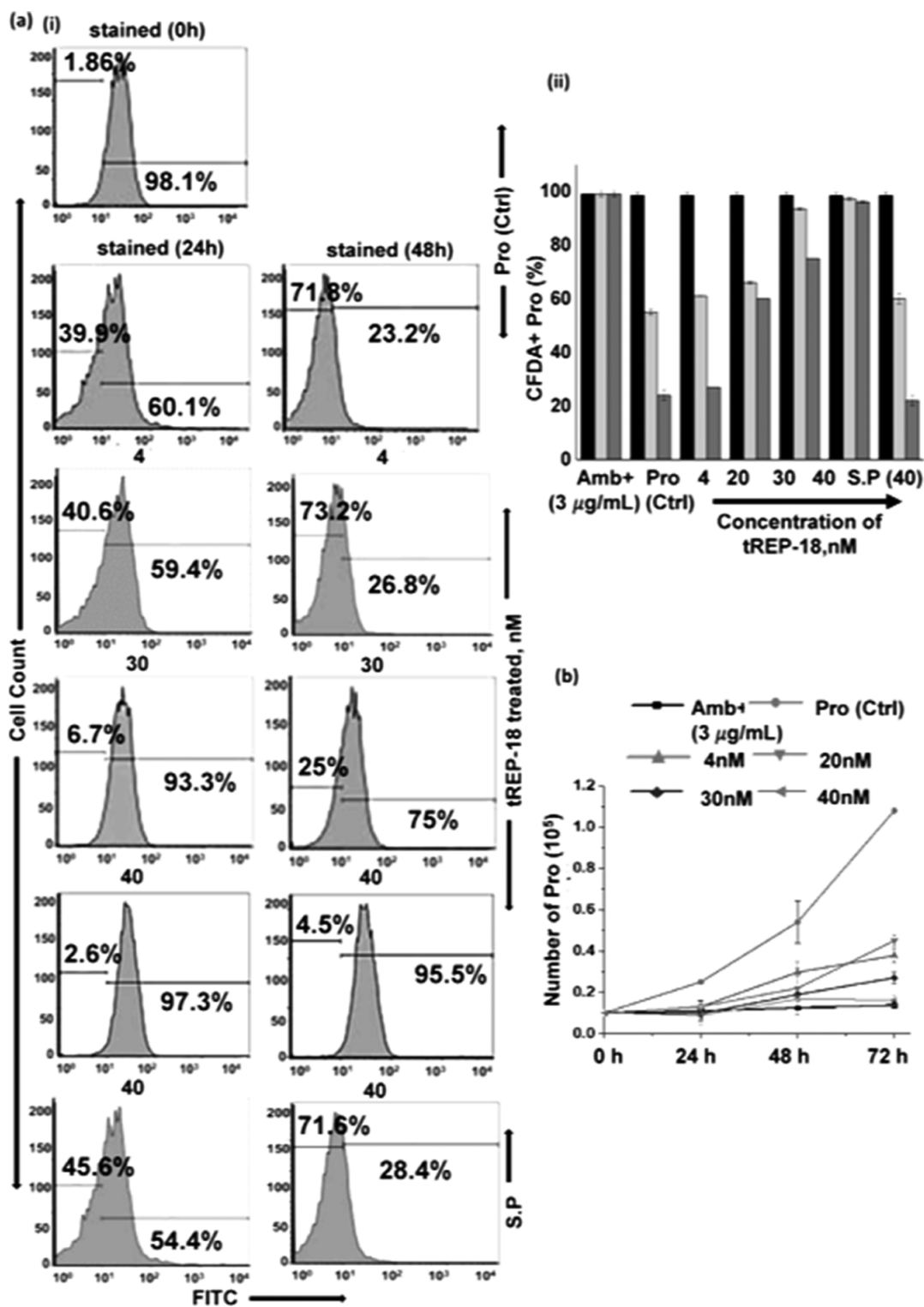
Figure 3. Effect of tREP-18 on the proliferation of promastigotes. [a(i)] Rate of proliferation was determined by the change in CFDA-SE-stained promastigotes as represented by flow cytometry histograms, depicting huge cellular multiplication arrest upon treatment with the 40 nM peptide at 24 and 48 h, respectively, Pro refers to untreated promastigotes; [a(ii)] nominal decrement observed in percentage of CFDA-SE positive promastigotes when treated by higher concentration of the tREP-18 peptide for 24 and 48 h; (b) increment in the number of trypan blue-stained parasites was evident following tREP-18 treatment in a dose-dependent manner; $n = 3$, *p-value < 0.05 was considered significant.

peptides in the antiparasitic database [Figure 1b]. The total energy was calculated using the FoldX tool, which uses the 3D structure of the peptide and provides quantitative estimation of the importance of the interactions contributing to the stability of the peptide, and the E-value was obtained from the

similarity search against the antiparasitic database. As a negative control, a scrambled form of tREP-18 was computationally designed, synthesized, and experimentally tested [Figure 1c]. The binding efficiency of tREP-18 with the membrane of promastigotes was computationally predicted to

be relatively high (delta G energy score = −3.5 kcal/Mol, using the virtual membrane depth of 4.2 Å). The delta G energy is provided by the OPM server, which is calculated as a sum of two terms: (i) a solvent accessible surface area-dependent term that accounts for van der waals, H-bonding, and entropy of solvent molecules; and (ii) an electrostatic term that includes solvation energy of dipoles and ions, and the deionization penalty of ionizable groups in a nonpolar environment. A total of four residues were predicted to be involved in the binding, constituting alanine 1,4 (A), serine 2 (S), and valine 3 (V) [Figure 1d]. To evaluate the cytotoxic effects of tREP-18 on *L. donovani* Ag83 promastigotes, the standard LDH assay[22] was performed. The IC50 value of **tREP-18** was found to be 22.13 nM (Figure 1e). The CC50 evaluation of the peptide in J774.A1 cells was detected to be 275 μM [Table S2]. The concentration-dependent response of parasites to the tREP-18 peptide showed percent inhibition up to 66.21% at 40 nM concentration at 24 h, whereas the scrambled peptide demonstrated 22.37% at the same concentration [Figure 1e]. Promastigotes treated with amphotericin B, which was taken as a positive control, showed ∼95% growth inhibition. For calculating the IC50 value, a 1−100 nM range of concentration was taken into consideration. Thus, tREP-18 was found to have a potent antileishmanial effect.

3.2. tREP-18 Treatment Imposes Severe Depletion in Parasite Metabolic Viability Both in Time- and Dose-Dependent Manner.
A dose- and time-dependent release of LDH was observed when promastigote cells were treated with **tREP-18**. The maximum LDH release was observed at 72 h in amphotericin B treated promastigotes (Avg. O.D. 0.946), representing 100% cytotoxicity [Figure 2a(i)]. **tREP-18** was able to induce the highest level of cytotoxicity (up to 92.83%) at 40 nM at 72 h vis-à-vis LDH release at 48 and 24 h, which showed 70.27 and 66.21%, respectively, while the scrambled peptide-treated samples showed 24.41% cytotoxicity at 72 h [Figure 2a(ii)]. Furthermore, to explore the mechanistic reasons for the increment of LDH levels that correlate with tREP-18-induced parasite growth inhibition, estimation of parasitic cell death was performed using the standard PI-based assay (Riccardi and Nicoletti, 2006). The highest percentage of PI positivity could be obtained at 72 h (95.5%) following treatment with 40 nM of tREP-18 concentration, similar to the level of cytotoxicity induced by amphotericin B treatment in promastigotes (positive control), which showed 97.6% of PI[POS] cells (Figure 2b). The results indicated a persistent reduction in parasite growth along with enhanced cell death as represented by the PI positivity against tREP-18 treatment.

3.3. tREP-18 Enforces Strong Antiproliferative Effect in *L. donovani* Promastigotes.
To further understand the impact of tREP-18 peptide treatment on cellular phenotype promastigotes, we studied promastigote proliferation using live staining with CFDA-SE (a strong membrane permeant dye) [Figure 3a(i,ii)]. The CFDA-SE dye, upon cleavage by esterases within the cell, generates reactive amine products that covalently bond with intracellular lysine to generate fluorescence. Based on this assay, it was inferred that tREP-18 could strongly attenuate the cell division/progression of promastigotes, while the scrambled peptide conferred hardly any impact. This finding was also supported by trypan blue exclusion assay-based determination of growth kinetics in tREP-18-treated parasites that showed significant enhancement in cell death [Figure 3b].

3.4. tREP-18 Treatment Causes Severe Membrane Distortion in Parasites.
After establishing the cytotoxic effect of **tREP-18** on Leishmania promastigotes, the detailed morphometric analysis of treated parasites was studied using SEM and AFM. At a 40 nM concentration of **tREP-18**, the swelling and rupture of promastigote membranes were observed compared to untreated parasites in SEM [Figure 4a]. Furthermore, AFM analysis unraveled profound alter-
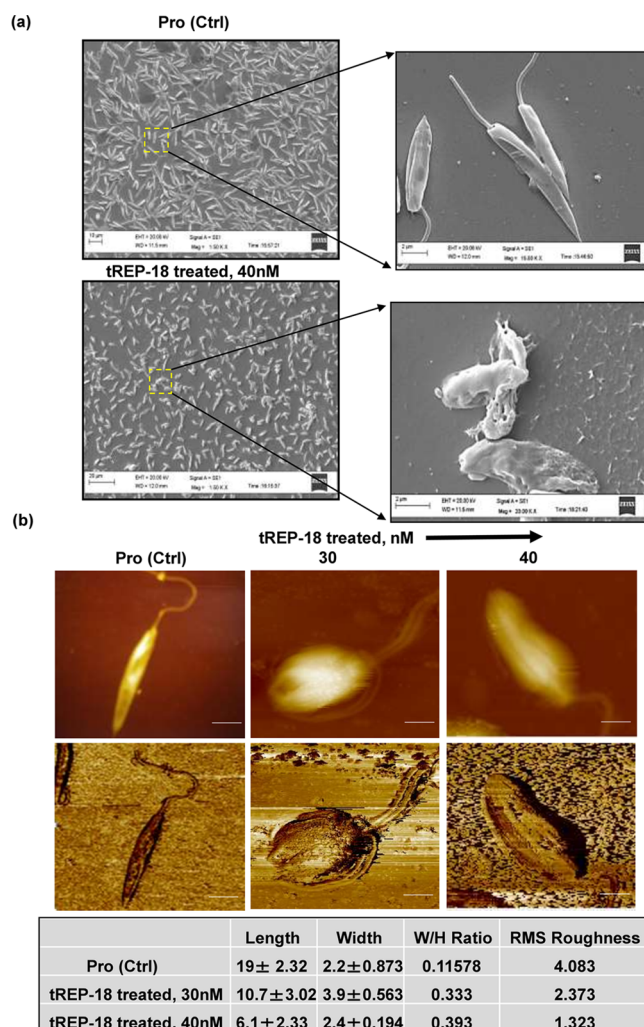

	Length	Width	W/H Ratio	RMS Roughness
Pro (Ctrl)	19± 2.32	2.2±0.873	0.11578	4.083
tREP-18 treated, 30nM	10.7±3.02	3.9±0.563	0.333	2.373
tREP-18 treated, 40nM	6.1±2.33	2.4±0.194	0.393	1.323

Figure 4. Surface topology and morphometric analysis of *L. donovani* promastigotes treated with tREP18. (a) Surface scanned micrographs of promastigotes in SEM at 1.5KX and 20.00KX magnifications demonstrated intact promastigotes in healthy control with constricted and disordered cellular architecture obtained in tREP-18-treated promastigotes; (b) AFM micrographs indicated severe topological alteration of the surface of tREP-18-treated promastigotes as compared to untreated promastigotes. The peptide treatment at 30 and 40 nM has drastically impaired the width (W) to height (H) ratio in treated parasites.

ations in membrane topology, including perturbed membrane architecture, constricted cellular structures, and shortened flagella, as denoted by substantial changes in the width (W) to height (H) ratio, from 0.1158 to 0.393 following treatment [Figure 4b]. Although the untreated promastigotes showed normal elongated spindle-shape parasites with an anterior and long flagellum. Additional surface topological analysis revealed a significant change of the RMS roughness value (R_q) of 4.083
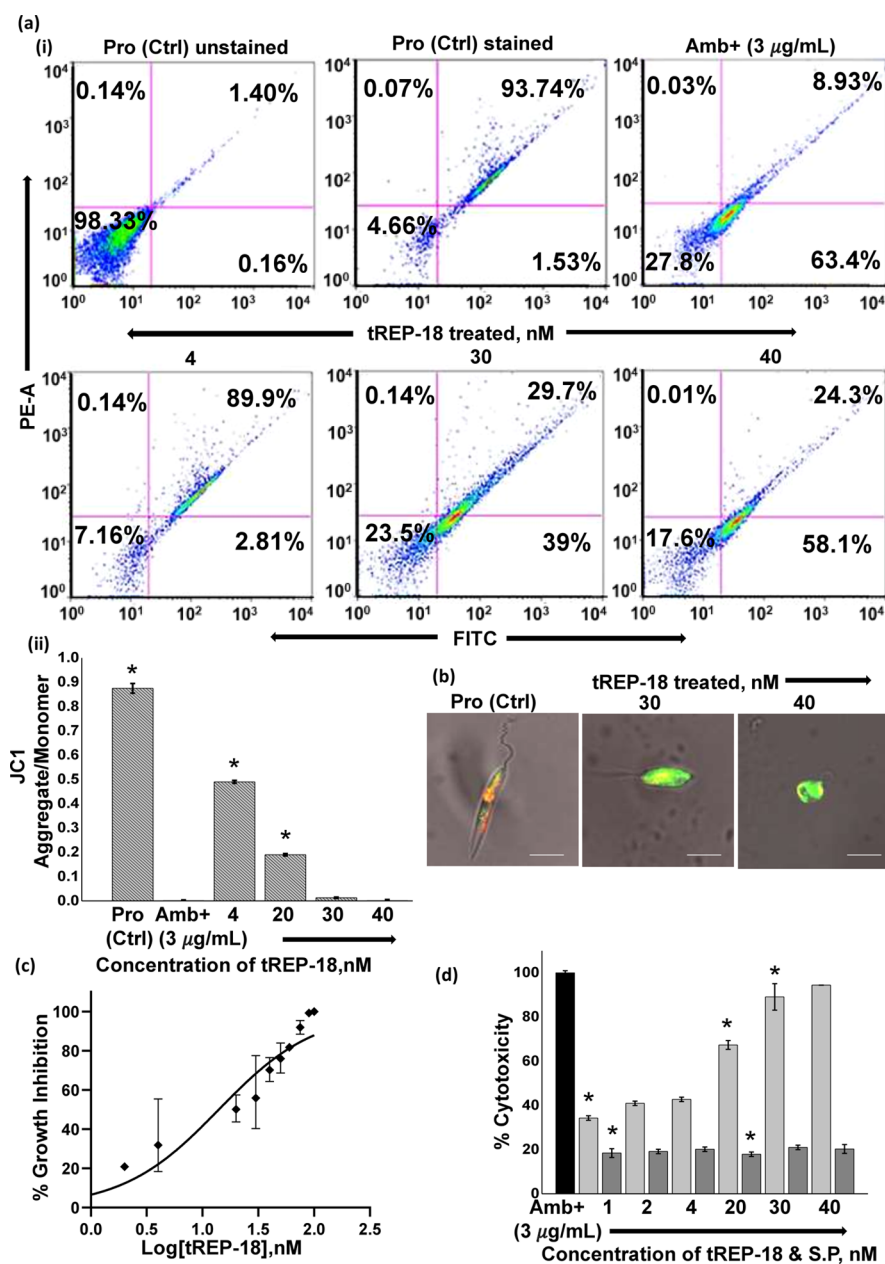
Figure 5. Effect of tREP-18 treatment on ΔΨm of Ag83 promastigotes and cytotoxic effect of tREP-18 on the PKDL strain. [a(i,ii)] Effect of the concentration-dependent treatment of tREP-18 on ΔΨm of Ag83 promastigotes indicated by the conversion in monomer to oligomer forms of JC-1 using flow cytometry histograms and confocal micrographs. The shift in intensity of red fluorescence (JC1 aggregates/PE) to green fluorescence (JC1 monomers/FITC) implies ΔΨm in promastigotes following tREP-18 treatment. The bar graphs denote the change in PE/FITC ratio corresponding to tREP-18-induced alterations in JC1 aggregate/monomer formation in promastigotes. The higher ratio refers to a healthy mitochondrial membrane and the lower ratio denotes destabilized membrane potential; (b) confocal micrographs depicted intense red fluorescence in control groups, whereas green fluorescence was observed in samples treated with peptides; (c) percentage inhibition was evaluated using the LDH assay for 24 h of tREP-18 treatment and IC50 was calculated using GraphPad prism; (d) cytotoxic effects of both tREP-18 and scrambled peptides on clinical PKDL isolate BS12 were determined, respectively, for 72 h; where $n = 3$, p-value < 0.05 indicated as * for all the experiments performed.

in the treated promastigotes as compared to a 1.323 value, indicating distorted membrane cytoskeleton.

3.5. tREP-18 Caused Disruption of the Mitochondrial Membrane and Destabilization of Redox Potential in *L. donovani*. Finally, to study the effect of **tREP-18** on the mitochondrial membrane potential (ΔΨm) of promastigotes, we have used a lipophilic, cationic dye (JC-1) exhibiting green fluorescence that enters the mitochondria and gets accumulated into a reversible complex oligomeric form, known as J aggregates emitting red fluorescence. This formation of J aggregates from its monomeric form depicts a healthy (ΔΨm) in parasites. Thus, to explore if **tREP-18** has any impact on ΔΨm of promastigotes, we have evaluated the change in fluorescence intensities using flow cytometry-based analysis and confocal imaging. In healthy untreated promastigotes, a PE/FITC ratio corresponding to a higher red to green ratio (0.87) was observed, representing hyperpolarised mitochondrion, suggesting a stable ΔΨm [Figure 5a(i)]. However, in the
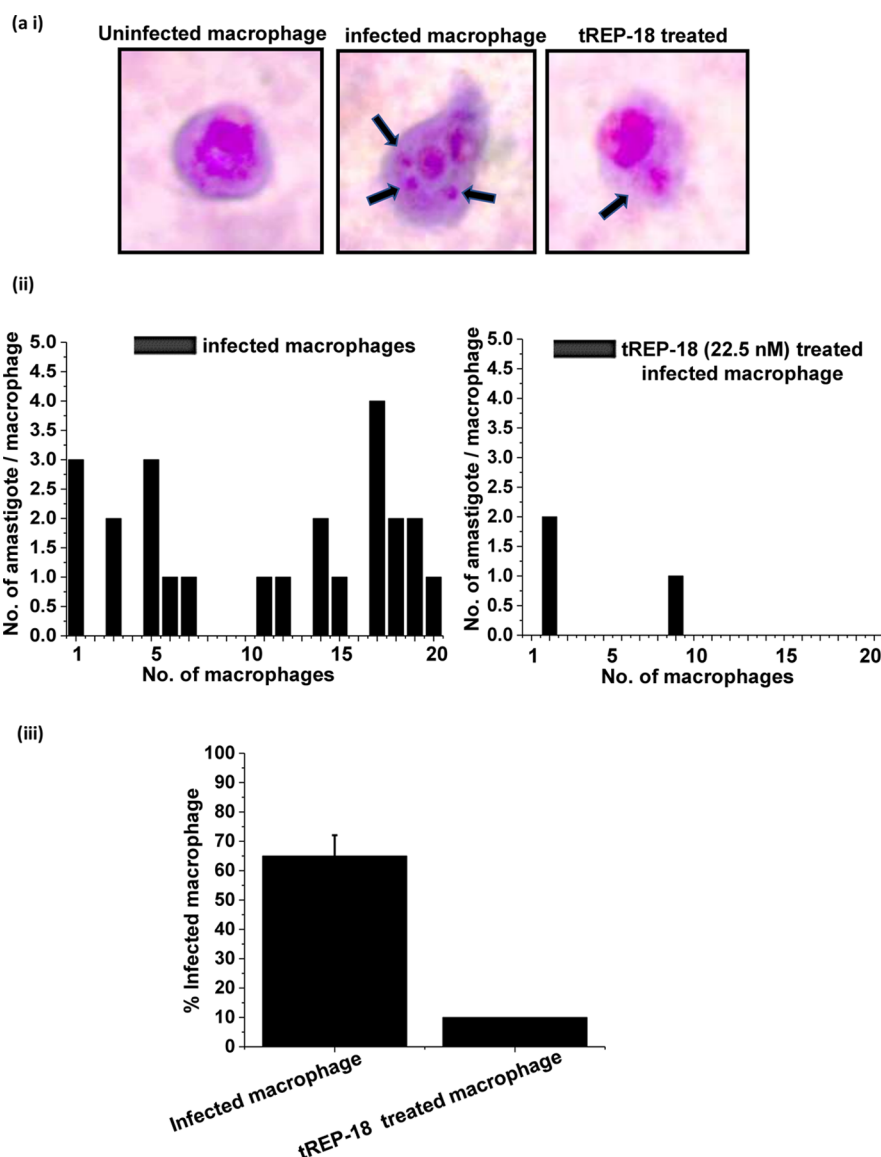
Figure 6. Leishmanicidal activity of tREP-18 against intramacrophage amastigotes. (a) Geimsa-stained images represented impact of tREP-18 treatment on mouse macrophages infected with *L. donovani* amastigotes; [a(ii)] bar graph represents the number of amastigotes per macrophage in both untreated and treated cells that were counted at a single cell level, where $n = 20$ distinct cells; [a)iii)] bar graph illustrates the percentage of infected macrophages for untreated and treated counterparts per six-well plates.

case of **tREP-18**-treated promastigotes, a drastic reduction in $\Delta\Psi m$ correlated with an increasing concentration of the peptide that could be matched with the amphotericin B treatment [Figure 5a(ii)]. The fluorescence signals were also evaluated using confocal microscopy. The confocal images represented enhanced levels of red fluorescence, which denotes more J aggregate formation due to higher $\Delta\Psi m$, whereas shifting toward lower red or accumulation of higher green fluorescence implies a strong indication of destabilized $\Delta\Psi m$. Notably, the mitochondrial uptake of JC-1 dye was found to decrease with **tREP-18** treatment as compared to healthy promastigotes, which was then manifested as stronger green fluorescence due to monomeric JC-1 formation. Intense red fluorescence was observed in control groups, suggesting JC-1 aggregation due to stable $\Delta\Psi m$, whereas green fluorescence was detected in treated samples [Figure 5b]. Based on this observation, it was inferred that **tREP-18** treatment leads to the disruption of the mitochondrial membrane structure.

Because PKDL can be life-threatening with the manifestation of disfiguring lesions leading to visceralization of organs,[23] we then evaluated the impact of both **tREP-18** and its scrambled form as a negative control, on the clinical isolate of the PKDL strain, BS12 of *Leishmania spp*. The **tREP-18** peptide demonstrated its potent antileishmanial efficacy as shown by its IC50 value (15 nM) in the PKDL strain [Figure 5c]. Based on the LDH assay results, the **tREP-18** treatment showed optimal toxicity at 1 nM with 34% cell death and maximum toxicity at 40 nM with 98% of death in PKDL promastigotes, comparable to the cytotoxic effect imposed by amphotericin B treatment [Figure 5d]. Whereas the scrambled peptide hardly showed any toxic effect for a period of 72 h. This data strongly suggests that **tREP-18** may adversely affect the metabolic cell viability of the BS12 strain of PKDL.

3.6. tREP-18-Treated *L. donovani* Demonstrated Significant Reduction in the Amastigote Model of Macrophage Infection. We further evaluated the cytotoxic
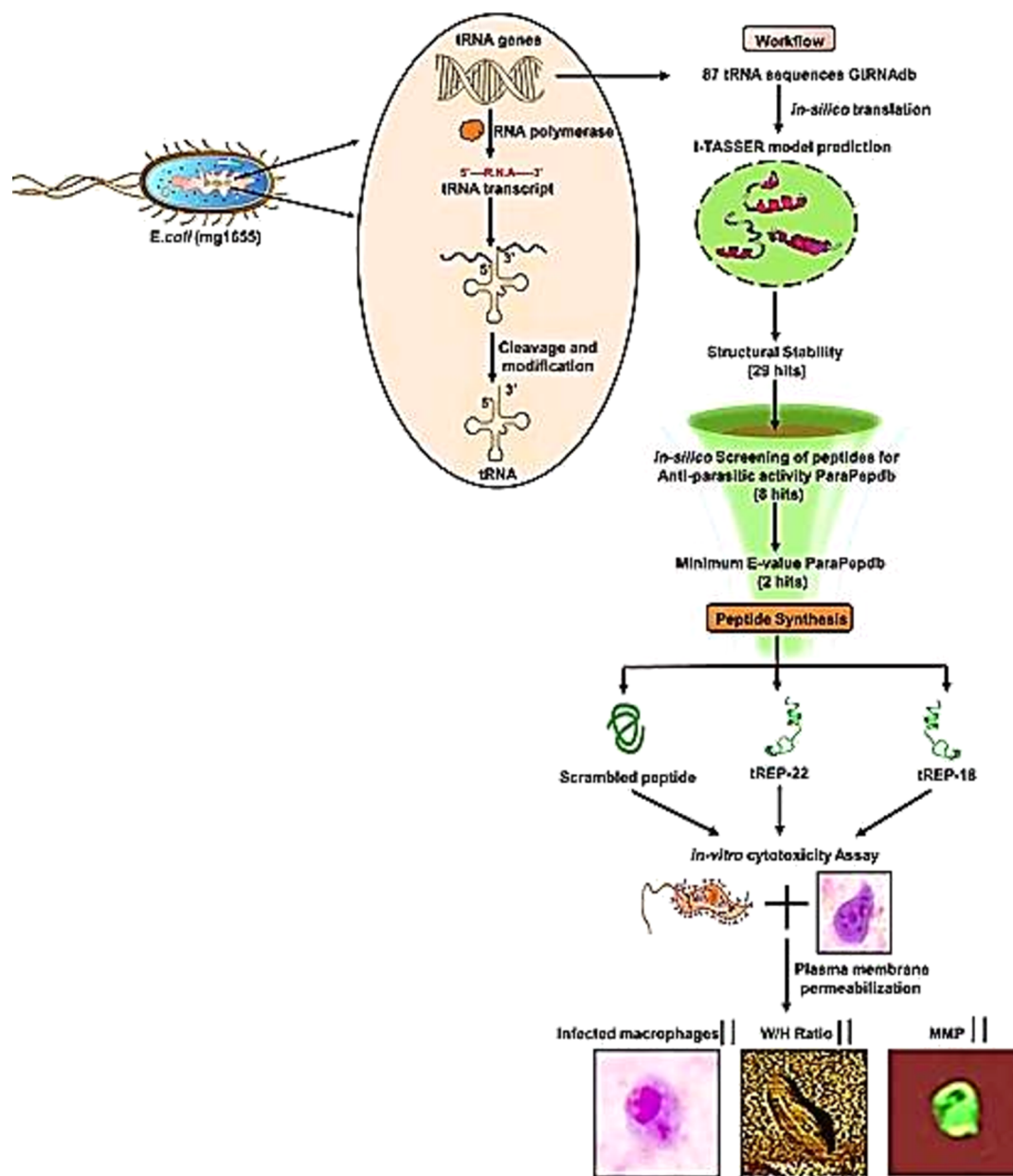
Figure 7. Working model for discovery and translational application of **tREP-18**.

effects of the peptide on infective intracellular amastigotes [Figure 6a(i)]. The number of amastigotes per infected macrophage was found to be predominantly reduced in **tREP-18**-treated samples (~1 amastigotes/macrophages), whereas control untreated macrophages had ~4 number of amastigotes/macrophages [Figure 6a(ii)]. The percentage of macrophages infected is also less following **tREP-18** treatment as compared to untreated control [Figure 6a(iii)]. The results clearly demonstrated **tREP-18** treatment has a pronounced effect on intracellular amastigotes in an exceptionally low micromolar range, suggesting its potential antileishmanial activity in both stages.

4. DISCUSSION

tRNAs are ancient molecular elements that predate full-fledged translational machinery. Although their primary evolutionary role has been to ferry amino acids to the ribosomal surface, some studies suggest that tRNAs may be recruited by some viruses for insertion and replicating purposes.[24] tRNA molecules have a monophyletic origin, with modern molecules derived from the universal translator. It is quite likely that cells may use the structural and functional flexibility of tRNAs to handle responsibilities that are beyond their traditional job descriptions. Taking into consideration this innate potential, here we provide the proof-of-the-concept of functional tRNA peptides as first-in-the-class molecules.

A total of 87 tRNA gene sequences from the *E. coli* genome (MG1655) were computationally translated into corresponding peptide sequence equivalents. All the hypothetical peptides were passed through a series of bioinformatics-based filters. A total of 29 stable peptides were generated from full-length translates for deeper in silico study. Out of 29 full-length peptides, tREP-18 was selected for experimental validation based on total energy and *E*-value (1.9) against an antiparasitic database [Table S1 and Figure 1a,b].

Suitable cell survival assays were designed to validate the predicted antiparasitic property of **tREP-18**. The **tREP-18** was also tested against several cancer cell lines and microbes but did not show any growth-influencing property. Interestingly, the IC50 value for **tREP-18** on *Leishmania* promastigotes was found to be 22.13 nM [Figure 1e]. The assessment of the CC50 value for **tREP-18**-treated J774.A1 cells was found to be 275 μM suggesting its nontoxic impact on the host macrophages [Table S2]. The in silico membrane binding studies revealed a relatively higher delta *G* energy score of −3.5 kcal/Mol for **tREP-18**, suggesting its probable interaction with parasite membrane proteins [Figure 1d], leading to an experimentally determined IC50 value [Figure 1e]. The significant tREP-18 IC50 and CC50 values encouraged further in vitro validation.

The LDH assay-based evaluation of **tREP-18**-induced cytotoxicity in promastigotes demonstrated a linear dose- and time-dependent correlation. This assay involved a cell death enzymatic marker that showed the maximal growth inhibitory impact of **tREP-18** at 40 nM, which drastically impairs the metabolic viability of promastigotes. This effect was found to closely match the effect of amphotericin B on growth of parasites at 72 h, whereas the scrambled peptide represented minimal cytoxicity for the same dose and time period [Figure 2].

Next, we asked if **tREP-18** treatment has any impact on the cellular proliferation of *L. donovani* promastigotes. To answer this, we performed a cell-based assay using CFDA-SE, a cell membrane permeable dye. The results demonstrated that **tREP-18** could significantly reduce the promastigote proliferation [Figure 3a(i,ii)]. These data were also strongly corroborated by the results obtained from a growth kinetic assay that showed a significant depletion in the number of promastigotes, suggesting enhanced cell death [Figure 3b].

Based on these readouts, we examined if tREP-18 would trigger any morphological changes in the membrane architecture of parasites. To answer this, we performed SEM- and AFM-based analysis of tREP-18-treated promastigotes. The high-resolution microscopic images show ultrastructural changes in the membranes of treated parasites, significant alteration in promastigotes morphology with visible loss in intercellular networking and ruptured cytoskeletal architecture [Figure 4a,b]. Collectively, observations indicate that **tREP-18** destabilized the cellular topology, causing intrusion in parent cell division and leading to growth arrest, which later induced parasite death.

To decipher the effect of **tREP-18** on mitochondrial membrane potential ($\Delta\Psi$m), an initial cellular event that has been reported as a marker of cell death in leishmania sp.,[25] we used a lipophilic cationic dye JC1 to understand $\Delta\Psi$m in treated parasites. In healthy cells, JC1 monomers can cross the mitochondrial membrane and get converted into a reversible oligomeric form of J aggregates that emit red fluorescence. This phenomenon was significantly affected in parasites treated at 40 nM **tREP-18** due to disrupted $\Delta\Psi$m. Thus, we assume that **tREP-18**-induced membrane destabilization is precedent to the impaired $\Delta\Psi$m. The disruption of $\Delta\Psi$m has been reported to generate reactive oxygen species, a direct hallmark of apoptosis [Figure 5a(i,ii),b, Table S3]. This finding was strongly corroborated by PI positive promastigotes as shown previously [Figure 2b(i,ii)].

We then asked whether **tREP-18** could show similar effects in the clinical form of *L. donovani* involved in PKDL manifestation. To resolve this query, we used the BS12 strain (clinical isolate of PKDL) for investigating the antileishmanial potential of the peptide using the LDH assay. As assumed, **tREP-18** demonstrated significant growth inhibition in BS12 at a much lower concentration of 18 nM ≥ IC50 [Figure 5c,d].

It is noteworthy that studies involved in the discovery of antileishmanial peptides have majorly focused on evaluating their activities against the promastigotes form of the parasite. However, recent advancements involving certain membrane-targeting antimicrobial peptides have been found to be effective for both promastigote and amastigote forms of parasite.[26] The efficacy of the **tREP-18** peptide on the *L. donovani* amastigotes was studied following treatment with **tREP-18** at 22.5 nM of concentration (∼IC50 value). A pronounced decrement in intracellular amastigotes was observed, suggesting high activity of the peptide against promastigote and amastigote forms [Figure 6]. Our results indicated **tREP-18** as a promising candidate for the development of anti-infective therapeutics targeting Leishmania. The details of the strategy have been explained in the working model [Figure 7].

In summary, to our best knowledge, this is the first report that demonstrates the emergence of a new class of functional molecules, that is, tRNA-encoded peptides (tREPs). In the future, it would be interesting to redesign tREPs from various organisms, build a library of tREPs, and study the structure and function relationship of tREPs. Overall, this work has laid a foundation for a new class of molecules and opened a new evolutionary window to explore deeper aspects of tREPs.

■ ASSOCIATED CONTENT

ⓈSupporting Information

The Supporting Information is available free of charge at https://pubs.acs.org/doi/10.1021/acsomega.2c00661.

> Computationally translated peptide sequences from *E. coli* tRNAs, toxicity of the tREP-18 peptide on mammalian cell lines, and dose-dependent effect on the mitochondrial membrane potential of tREP-18-treated promastigotes (PDF)

■ AUTHOR INFORMATION

Corresponding Authors

Soumya Pati — *Department of Life Sciences, Shiv Nadar University, Greater Noida 201314 Uttar Pradesh, India*; Phone: 0091 9560 916 013; Email: soumya.pati@snu.edu.in

Pawan Kumar Dhar — *School of Biotechnology, Jawaharlal Nehru University, New Delhi 110067, India; Special Centre for Systems Medicine, Jawaharlal Nehru University, New Delhi 110067, India*; ● orcid.org/0000-0002-4032-7679; Phone: 0091 9953 345 001; Email: pawandhar@mail.jnu.ac.in

Shailja Singh — *Special Centre for Molecular Medicine, Jawaharlal Nehru University, New Delhi 110067, India*; ● orcid.org/0000-0001-5286-6605; Phone: 0091 9868 512 025; Email: shailjasingh@mail.jnu.ac.in

Authors

Amrita Chakrabarti — *Department of Life Sciences, Shiv Nadar University, Greater Noida 201314 Uttar Pradesh, India; Special Centre for Molecular Medicine, Jawaharlal Nehru University, New Delhi 110067, India*

Monika Kaushik − *School of Biotechnology, Jawaharlal Nehru University, New Delhi 110067, India*

Juveria Khan − *School of Biotechnology, Jawaharlal Nehru University, New Delhi 110067, India*

Deepanshu Soota − *National Centre for Biological Sciences, Bangalore 560065, India*

Kalairasan Ponnusamy − *National Centre for Disease Control, New Delhi 110054, India*

Sunil Saini − *Department of Biophysics, All India Institute of Medical Sciences, New Delhi 110029, India*

Siddharth Manvati − *School of Biotechnology, Jawaharlal Nehru University, New Delhi 110067, India*

Jhalak Singhal − *Special Centre for Molecular Medicine, Jawaharlal Nehru University, New Delhi 110067, India*

Anand Ranganathan − *Special Centre for Molecular Medicine, Jawaharlal Nehru University, New Delhi 110067, India*

Complete contact information is available at:
https://pubs.acs.org/10.1021/acsomega.2c00661

Author Contributions

P.K.D. conceived the original idea of making the functional peptides from tRNA, led computational studies, and peptide synthesis, and drafted the first version of the manuscript. M.K., J.K., S.M., D.S., K.P., S.S. (Saini), and S.S. (Singh) were involved in bioinformatics analyses of tREPs at various stages. A.C. performed all the biological experiments described in this paper. A.C. and J.S. performed preliminary analyses and in silico membrane binding studie, and prepared the initial draft. S.S. (Singh) and S.P. conceived the experimental work plan for Leishmania, supervised the experiments, and troubleshooted and analyzed the data. A.R. performed the data analysis. A.C. and S.P. wrote the final draft. S.S. (Singh), S.P., and P.K.D edited the final version of the manuscript.

Notes

The authors declare no competing financial interest.

■ REFERENCES

(1) Sharp, S. J.; Schaack, J.; Cooley, L.; Burke, D. J.; Soil, D. Structure and transcription of eukaryotic tRNA gene. *Crit. Rev. Biochem. Mol. Biol.* **1985**, *19*, 107−144.

(2) Di Giulio, M. The origin of the tRNA molecule: Implications for the origin of protein synthesis. *J. Theor. Biol.* **2004**, *226*, 89−93.

(3) Rodin, A. S.; Szathmáry, E.; Rodin, S. N. On origin of genetic code and tRNA before translation. *Biol. Direct* **2011**, *6*, 14.

(4) Sugahara, J.; Kikuta, K.; Fujishima, K.; Yachie, N.; Tomita, M.; Kanai, A. Comprehensive Analysis of Archaeal tRNA Genes Reveals Rapid Increase of tRNA Introns in the Order Thermoproteales. *Mol. Biol. Evol.* **2008**, *25*, 2709−2716.

(5) Randau, L.; Münch, R.; Hohn, M. J.; Jahn, D.; Söll, D. Nanoarchaeum equitans creates functional tRNAs from separate genes for their 5′- and 3′-halves. *Nature* **2005**, *433*, 537−541.

(6) Fujishima, K.; Sugahara, J.; Kikuta, K.; Hirano, R.; Sato, A.; Tomita, M.; et al. Tri-split tRNA is a transfer RNA made from 3 transcripts that provides insight into the evolution of fragmented tRNAs in archaea. *Proc. Natl. Acad. Sci. U.S.A.* **2009**, *106*, 2683−2687.

(7) Soma, A.; Onodera, A.; Sugahara, J.; Kanai, A.; Yachie, N.; Tomita, M.; et al. Permuted tRNA genes expressed via a circular RNA intermediate in Cyanidioschyzon merolae. *Science* **2007**, *318*, 450−453.

(8) Fujishima, K.; Kanai, A. tRNA gene diversity in the three domains of life. *Front. Genet.* **2014**, *5*, 142.

(9) Kanai, A. Disrupted tRNA genes and tRNA fragments: A perspective on tRNA gene evolution. *Life* **2015**, *5*, 321−331.

(10) Shen, Y.; Yu, X.; Zhu, L.; Li, T.; Yan, Z.; Guo, J. Transfer RNA-derived fragments and tRNA halves: biogenesis, biological functions and their roles in diseases. *J. Mol. Med.* **2018**, *96*, 1167−1176.

(11) Madeira, F.; Park, Y. m.; Lee, J.; Buso, N.; Gur, T.; Madhusoodanan, N.; Basutkar, P.; Tivey, A. R. N.; Potter, S. C.; Finn, R. D.; Lopez, R. The EMBL-EBI search and sequence analysis tools APIs in 2019. *Nucleic Acids Res* **2019**, *47*, W636−W641.

(12) Kelley, L. A.; Mezulis, S.; Yates, C. M.; Wass, M. N.; Sternberg, M. J. E. The Phyre2 web portal for protein modeling, prediction and analysis. *Nat. Protoc.* **2015**, *10*, 845−858.

(13) Van Der Spoel, D.; Lindahl, E.; Hess, B.; Groenhof, G.; Mark, A. E.; Berendsen, H. J. C. GROMACS: fast, flexible, and free. *J. Comput. Chem.* **2005**, *26*, 1701−1718.

(14) Laskowski, R. A.; MacArthur, M. W.; Moss, D. S.; Thornton, J. M. PROCHECK: a program to check the stereochemical quality of protein structures. *J. Appl. Cryst.* **1993**, *26*, 283−291.

(15) Schymkowitz, J.; Borg, J.; Stricher, F.; Nys, R.; Rousseau, F.; Serrano, L. The FoldX web server: an online force field. *Nucleic Acids Res* **2005**, *33*, W382−W388.

(16) Mehta, D.; Anand, P.; Kumar, V.; Joshi, A.; Mathur, D.; Singh, S.; Tuknait, A.; Chaudhary, K.; Gautam, S. K.; Gautam, A.; Varshney, G. C.; Raghava, G. P. S. ParaPep: a web resource for experimentally validated antiparasitic peptide sequences and their structures. *Database* **2014**, *2014*, bau051.

(17) Lomize, M. A.; Lomize, A. L.; Pogozheva, I. D.; Mosberg, H. I. OPM: orientations of proteins in membranes database. *Bioinformatics* **2006**, *22*, 623−625.

(18) Prajapati, V. K.; Sundar, S.; Ostyn, B.; Dujardin, J.-C.; Vanaerschot, M.; Rai, M.; et al. In vitro susceptibility of Leishmania donovani to miltefosine in Indian visceral leishmaniasis. *Am. J. Trop. Med. Hyg.* **2013**, *89*, 750−754.

(19) Ahuja, K.; Arora, G.; Khare, P.; Selvapandiyan, A. Selective elimination of Leptomonas from the in vitro co-culture with Leishmania. *Parasitol. Int.* **2015**, *64*, 1−5.

(20) Gluenz, E.; Wheeler, R. J.; Hughes, L.; Vaughan, S. Scanning and three-dimensional electron microscopy methods for the study of Trypanosoma brucei and Leishmania mexicana flagella. *Methods Cell Biol.* **2015**, *127*, 509−542.

(21) Sivandzade, F.; Bhalerao, A.; Cucullo, L. Analysis of the Mitochondrial Membrane Potential Using the Cationic JC-1 Dye as a Sensitive Fluorescent Probe. *Bio-Protoc.* **2019**, *9*, No. e3128.

(22) Korhonen, E.; Rönkkö, S.; Hillebrand, S.; Riikonen, J.; Xu, W.; Järvinen, K.; et al. Cytotoxicity assessment of porous silicon microparticles for ocular drug delivery. *Eur. J. Pharm. Biopharm.* **2016**, *100*, 1−8.

(23) Sengupta, R.; Chaudhuri, S. J.; Moulik, S.; Ghosh, M. K.; Saha, B.; Das, N. K.; et al. Active surveillance identified a neglected burden of macular cases of Post Kala-azar Dermal Leishmaniasis in West Bengal. *PLoS Neglected Trop. Dis.* **2019**, *13*, No. e0007249.

(24) Mak, J.; Kleiman, L. Primer tRNAs for Reverse Transcription. *J. Virol.* **1997**, *71*, 8087−8095.

(25) Riccardi, C.; Nicoletti, I. Analysis of apoptosis by propidium iodide staining and flow cytometry. *Nat. Protoc.* **2006**, *1*, 1458−1461.

(26) Khalili, S.; Mohebali, M.; Ebrahimzadeh, E.; Shayan, P.; Mohammadi-Yeganeh, S.; Moghaddam, M. M.; et al. Antimicrobial activity of an antimicrobial peptide against amastigote forms of Leishmania major. *Vet. Res. Forum* **2018**, *9*, 323−328.